LiM 2011

Ultrafast scan techniques for 3D-µm structuring of metal surfaces with high repetitive ps-laser pulses

Stephan Bruening[a], Guido Hennig[b], Stephan Eifel[c], Arnold Gillner[c]

[a] *Fa. Schepers GmbH & CO KG*
[b] *Fa. Daetwyler Graphics AG*
[c] *Fraunhofer ILT, Aachen*

Short Abstract

Metals and other materials can be machined with surpassing quality and highest flexibility with high power ultrafast lasers. In this study a slab based MOPA ps-laser system with fluencies of up to 30 J/cm² and pulse repetition rates in the multi MHz range for processing of large embossing metal rollers has been investigated. Different materials (Cu, Ni, Al, steel) have been explored for parameters like ablation rate per pulse, ablation geometry, surface roughness, influence of pulse overlap and number of loops. An enhanced ablation quality and an effective ablation rate of 4 mm³/min has been achieved by using different scanning systems and an optimized processing strategy.

Keywords: ultrashort laser pulse, 3D µm machining, ablation, acousto optical deflector (AOD), polygon

1. Motivation / State of the Art

3D micro-structuring of large scale metal surfaces for embossing and printing applications with ps-lasers is boosted by the availability of new high power ultrashort pulse laser sources allowing short processing times. Despite the fact that machining with ultrashort laser pulses offer higher precision, the technology is still not being used in the industry for large scale parts as ultra short laser ablation is still lacking productivity with an magnitude smaller ablation rate compared to the ns-laser pulse ablation. Approaches to use a combination of a fast but non-accurate ns-laser ablation followed by picoseconds-fine processing have not been successful with regard to accuracy. In Fig. 1 the ablation (diameter approx. 10µm) with single laser pulses with a 1 ns laser and a pulse energy of 10µJ shows dynamical material movements in the ablation zone. A ring of melt and recast material is visible which limits the achievable resolution of this process.

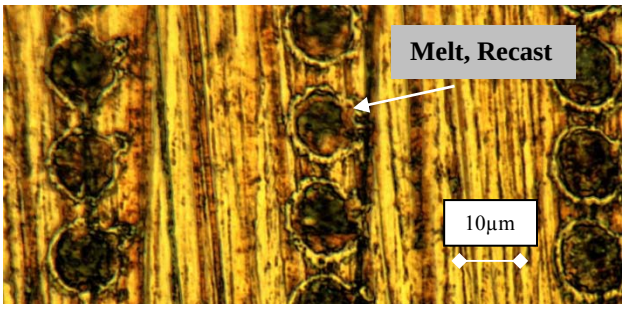

Fig. 1 Cu, single pulse, 1ns laser, 10µJ pulse energy, 10µm diameter

In order to achieve very high ablation qualities the accumulation of surface defects due to laser processing e.g. surface roughness, debris and fluid-dynamical movements of melt must be avoided right from the beginning of the process. This can be achieved by processing layer to layer with the same high quality of the almost cold ablation by

ultrashort laser pulses. However, this concept requires an efficient engraving algorithm with well-balanced process parameters to achieve highest precision and maximized ablation rate, which has been evaluated in previous experiments [1]. As a result, it can be stated that in order to preserve the optimized processing conditions at higher power levels, the repetition rate must be increased and the fluencies must be kept moderate. The available pulse repetition rates of ps-lasers in the MHz range and the relatively slow scanning speed of common galvanometric scan devices in the range of 5 m/s imply a large pulse overlap. This leads to a high local thermal accumulation and a pulse-plasma interaction on the metal surface [2] leading to a decreased machining quality that can be classified between ps- and ns-pulse regimes [6]. In order to enable the use of high pulse repetition rates with less thermal effects, an ultrafast scanning technique is required. Within this publication two different scan approaches for high scan speeds (up to 100 m/s) have been evaluated by means of scanning large area surfaces for embossing or printing applications.

If large scan angles (e.g. 10° or more) with lower line frequencies (some 10 kHz) are of interest, a polygon wheel is the first choice. For high line frequencies (some 100 kHz) with smaller angles (< 2°) AOD´s (acousto optical deflectors) can be used. The most efficient way is to use a combination of a fast axis (to adjust the desired spatial pulse to pulse distance) with a low scanning speed device for the perpendicular direction. In our case, a commercial cylinder engraving system with high circumferential speeds (30-40 m/s) of the cylinder has been combined with an even faster AOD system which allows a scan of the beam perpendicular to the rotation of the cylinder. In the following this scan principle will be referred to as “cross scan”. With this system a reasonable use of high repetitive ps-lasers in the multi MHz-regime with respect to processing speeds and ablation quality is possible. By adjusting the pulse overlap to an optimal value, high average laser power can be used by simultaneously keeping the same quality standard known from low repetitive ps-lasers. This study includes the analysis of structured areas from spot size dimensions of 10µm up to several hundred microns on two- and three-dimensional geometries.

2. Experimental studies of high repetitive ultra short pulse laser material processing

The ps-laser ablation studies have been performed with two different beam delivery approaches. In the first approach, the laser spot was moved by a slow feed along the axis of a fast rotating cylinder (cf. section 2.1). Fig. 2 shows the machine design with a rotating cylinder between two tail stocks. The ps-laser is mounted on a carriage that moves along the cylinder axis controlled by the data flow. The rotational symmetry of the cylinder allows fast and constant scanning speeds of up to 40 m/s even with heavy cylinders with lengths of up to 8 m and diameters of up to 1.2 m.

In the second approach a special algorithm was tested using a fast scanned laser spot and a slowly rotating cylinder (cf. section 2.2).

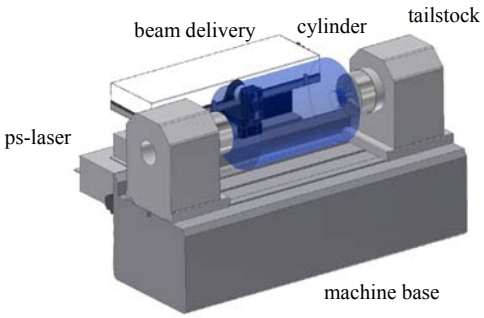

Fig. 2 Cylinder laser-micro-machining device

For the experiments a new developed ps-laser with repetition rates of up to 3.3 MHz and an average power of 80W has been used. Using a fast rotating work piece (cylinder) for pulse separation, the maximum usable laser power and thereby the maximum ablation rate is limited by the maximum rotation speed of the machine (Fig. 3). For even higher ablation rates, additionally a fast beam movement must be introduced to achieve the spatial separation of the pulses. This could allow to use pulse repetition rates in the >10 MHz range with high quality and the ablation rate could be increased by one order of magnitude.

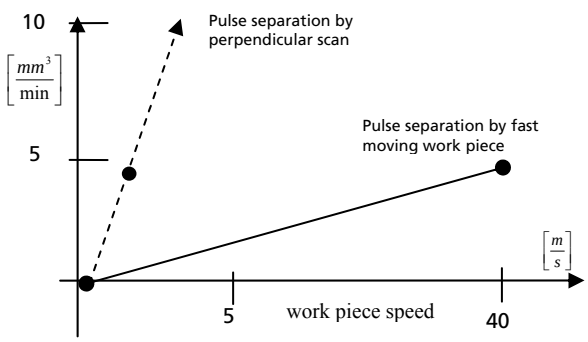

Fig. 3 Theoretical ablation rate by type of beam separation

2.1. Pulse separation by a fast rotating work piece

Common cylinder engraving systems already allow parameter studies with different pulse overlaps without using a rotating polygon or an AOD device. A benefit of this approach is the high synchronism of the fast cylinder rotation which allows high precision. While the laser spot is moving relatively slow (1-5 mm/s) along the cylinder axis, the rotating cylinder defines the scanning speed. With this method, the pulses of a ps-laser with 2 MHz repetition rate and a spot diameter of 15µm can be placed on the surface of the cylinder without pulse to pulse interaction (without pulse overlap in *direction of circumference of the cylinder*). By altering the rotation speed of the cylinder the overlap between two consecutive pulses can easily be adjusted. The time for one rotation is in the ms-range so that the pulse overlap in axial direction has no effect on the ablation process itself (e.g. thermal effects). This allows the local accumulation of many pulses by keeping the precision of the ultra-short ablation process at the same time. The ablation behavior of different metals (Cu, Ni, Al, steel) has been investigated by engraving squared rotogravure cells with a diagonal diameter of 150µm (Fig.7). Depending on the sort of metal, ablation rates of up to 4 mm³/min with resolutions of up to 5080 dpi were achieved.

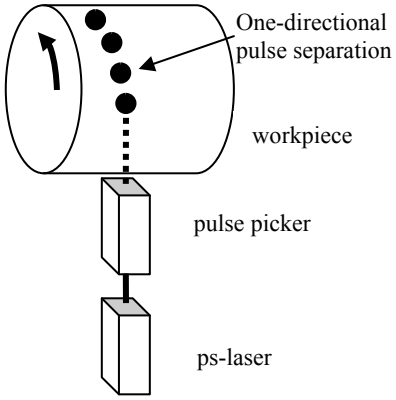

Fig. 4 beam separation by a fast moving workpiece

2.2. Pulse separation by a combination of cylinder rotation & perpendicular scanning (cross scan technique)

In order to guarantee an efficient and precise ultra fast ablation process without thermal effects at pulse repetition rates higher than 10MHz, an ultra fast, precisely controlled and reproducible beam positioning algorithm is required in order to distribute the sequence of pulses spatially on the cylinder surface (Fig. 5). An important point is the development of a fast cross scan setup using devices like rotating polygons or AOD's which allow to move the laser spot with speeds over 100 m/s. Fast writing of cross scan lines with ps-laser pulses have been realized with an AOD at 40 m/s by applying a chirped RF-frequency to the acousto-optical cell. The deflection angle Θ of the AOD is within the range of some mrad. The lines have been synchronized with the cylinder revolution which was an order of magnitude slower than the cross-scan speed. The time scheme of the frequency chirp of the AOD signal defines the position and the speed of the spot on the work piece. For the evaluation of the fundamental influencing factors and parameters the cross-scan line has been investigated by variation of line frequency, chirp time, depth of focus and fluence using the feed forward scheme shown in section 3.2.

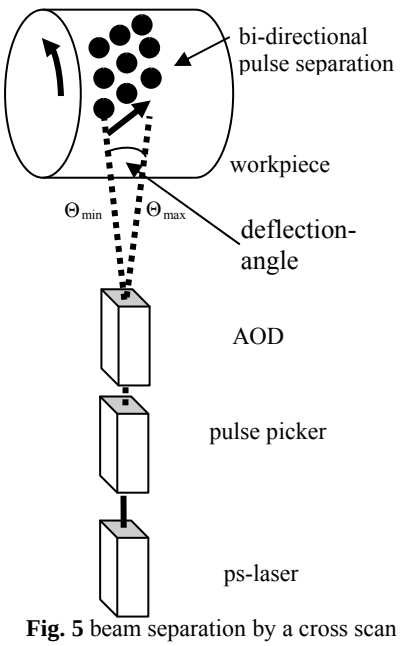

Fig. 5 beam separation by a cross scan

3. Results

3.1 Pulse separation by a fast rotating work piece

3.1.1 Ablation rate with respect to fluence and pulse overlap

The ablation rate depends on the applied fluence F_x with respect to the specific threshold fluence F_{th} of the material and is limited by the material dependent thermal penetration depth d of the pulse. The experimental ablation rates have been evaluated by engraving 150µm² cells as shown in Fig. 7 These cells have been ablated with different

fluencies (0.5, 3, 6, 10 and 13 J/cm², adjusted by an external pulse picker) and machined with 8 different scanning speeds (3-24 m/s). The results of this investigation are shown in Fig. 6 a) and 6 b). For low scanning speeds with high pulse overlap an increased ablation rate has been observed, induced by an enhanced pulse to pulse interaction

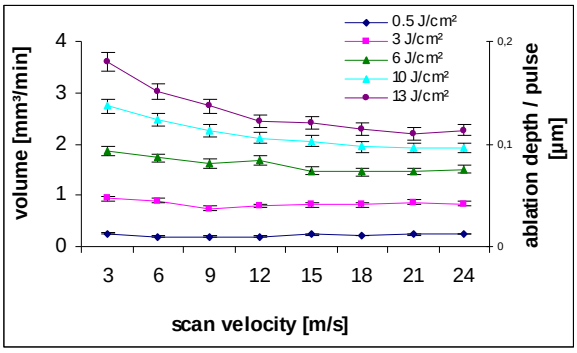

Fig. 6 a) Influence pulse – pulse interaction to the ablation rate, Cu

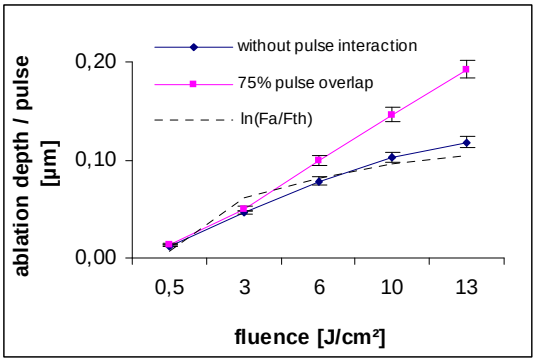

Fig. 6 b) Penetration depth per pulse, Cu

or pre-heating effect. Similar effects could already be demonstrated with pulse burst techniques [6]. This leads to higher penetration depths compared to the dashed curve (in Fig. 6 b) which shows the well known theoretical logarithmical behaviour of the ablation depth L for increasing laser pulse fluence F_x as for example described in [1]. Besides to the ablation rate, the contour accuracy between the digital image data and the produced geometries is a major point when comparing the characteristics of the picosecond approach with the nanosecond processes. It can be found that the pulse overlap has a significant influence on the quality of the processed cells as shown in Fig. 7. All examples are processed with the same fluence of 13J/cm^2.

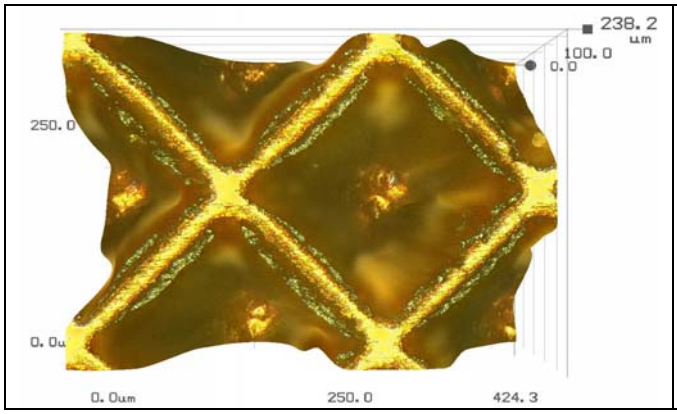

Fig. 7 a) Cu cell, Scan velocity: 3m/s, pulse-pulse overlap: 75%

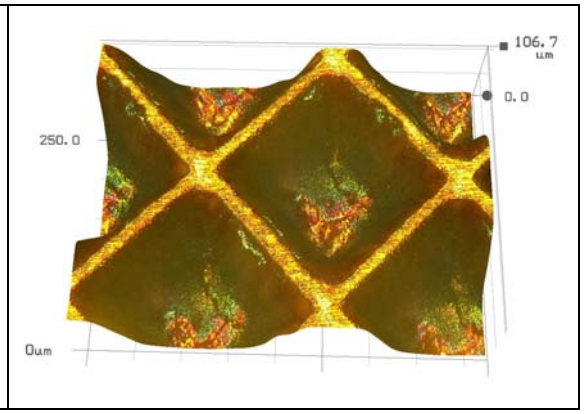

Fig. 7 b) Cu cell, Scan velocity: 12m/s, pulse-pulse overlap: 50%

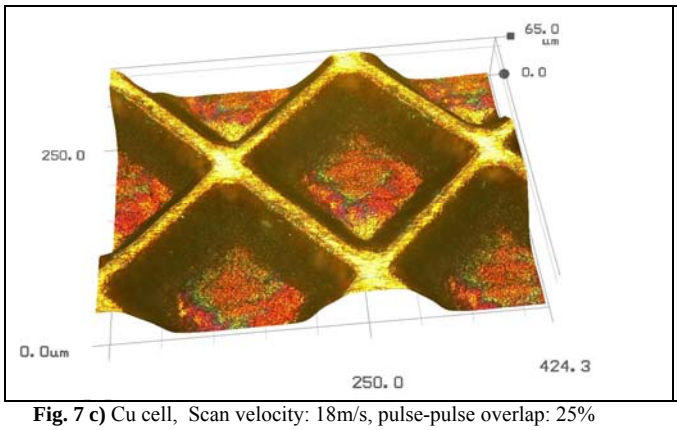

Fig. 7 c) Cu cell, Scan velocity: 18m/s, pulse-pulse overlap: 25%

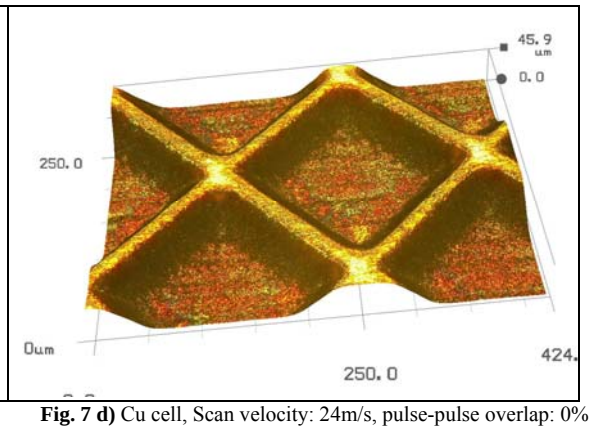

Fig. 7 d) Cu cell, Scan velocity: 24m/s, pulse-pulse overlap: 0%

For a pulse overlap of 75% (Fig. 7 a)) the ablated surface is covered with artefacts, typical for a melt-dominated ablation process: oxide residues, burrs and an uneven bottom. However for decreasing pulse overlaps the laser ablated structure converges to the structure, which is defined by the digital data set (Fig. 7b, 7c, 7d)). The structure processed with a pulse overlap of 25% shows minor thermal influences, identificable through the annealing colors at the bottom of the cells. Finally Fig. 7 d) (0% pulse overlap) shows a structure without any artefacts. This parameter study shows the tradeoff between the decreasing quality of the structure and an increased ablation rate caused by an enhanced pulse to pulse interaction. The achieved qualities in Fig. 7 a) and 7 b) are comparable with the processing quality of ns-lasers. Consequently high power picosecond laser pulses allows to produce structures with much higher qualities than with ns-pulses, if the pulse to pulse overlap is optimized (Fig. 8).

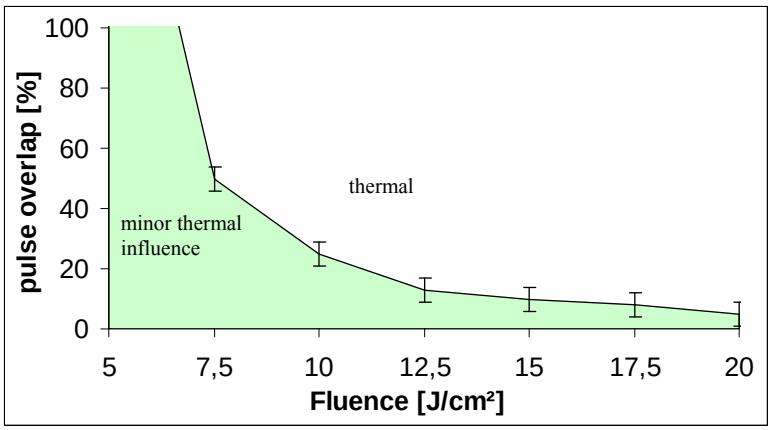

Fig. 8 Process diagram of the optimal parameters for Cu at 2MHz

3.1.2 Resolution

In printing applications the spatial resolution is defined by the information density and the accuracy of the digital data transfer and the size of the laser spot. The experimental studies were done with a Gaussian beam profile. For a given focus diameter w_0 (1/e²) the effective spot size can be calculated as follows [4]:

$$D_{focus}^2 = 2w_0^2 \ln\left[\frac{F_x}{F_{th}}\right] \qquad (1.0)$$

The effective measured ablation diameter for one pulse on a copper surface was determinated for different fluencies as shown in Fig. 9 a). The horizontal line represents a focused diffraction limited laser beam and the dashed line the trend of the relation (1.0).

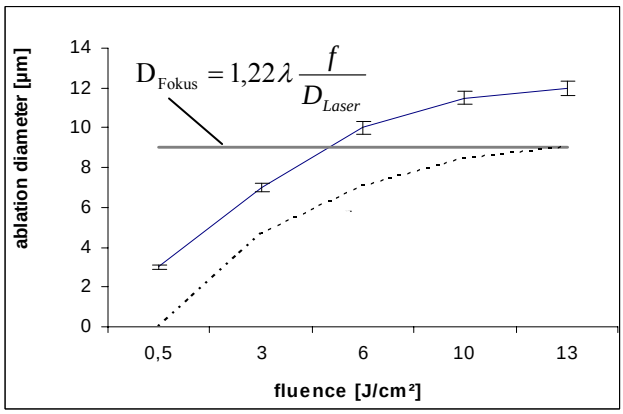

Fig 9 a) Ablation diameter vs. Fluence in Cu

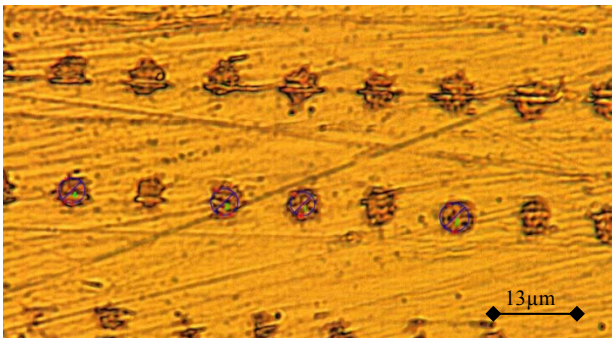

Fig. 9 b) Cu, 0.5 J/cm², 1 pulse, ablation diameter 3µm

In Fig. 9 b) the ablated spots for single pulses at a fluence of 0.5 J/cm² are shown. The diameter of 3µm is below the diameter of the diffraction limited laser beam. At this small fluence only the tip of the Gaussian profile is above the threshold for ablation. This allows to structure cell geometries below the diffraction limit. Compared to the ablation

process in ns-laser processing which is dominated by melting, the ablation with a ps-laser allows for a finer resolution.

3.1.3 Surface roughness

For a high precision 3D structuring process, a constant surface roughness is important, independent from the structure depth. The surface roughness was investigated by varying two different parameters, the Fluence F and the ablation depth. In a first step the surface roughness has been observed in dependence of the ablation depth in terms of the number of consecutively ablated layers and at constant parameters of the laser and the machine. The processed structures have been squared fields of 15 x 15mm² with a maximum depth of 200 µm (Fig. 10 a). The surface roughness shows different results in axial and circumferential direction. In circumferential direction the laser pulses are placed in an unsynchronized stochastically way, which gives a process of ongoing smoothing for consecutive layers. With this process the roughness can be kept as small as Ra = 0.1µm. In axial direction, the positioning of the laser spot was exactly on the same position from layer to layer. This induces an increasing surface roughness with ongoing depth. This could be avoided by a stochastically change of the start position from layer to layer. In Fig. 10 b) the surface roughness is shown in dependence of the fluence. The surface roughness is decreasing with the fluence, for both (axial and circumferential) direction due to an enhanced ablation spot diameter, which leads to more overlap of the spots with reduced residual parts according to less roughness.

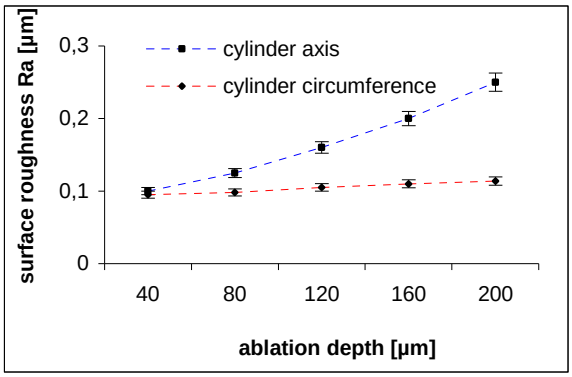

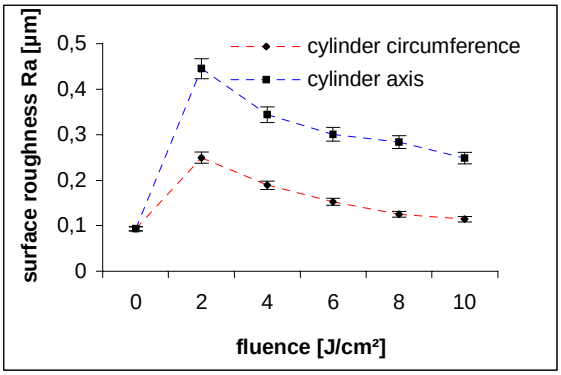

Fig. 10 a) surface roughness in dependence to the structure depth, Cu

Fig. 10 b) surface roughness in dependence to the fluene, Cu

3.1.4 Comparison of different materials

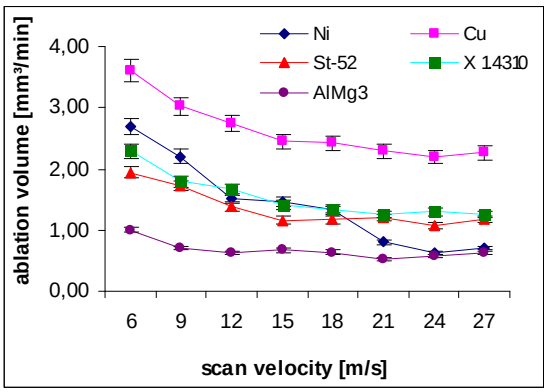

Fig. 11 ablation rate comparison of different metals

The investigation, presented in section 3.1.1 was analogous performed with different materials: nickel, copper, steel St-52, stainless steel X 1.4310 and AlMg3. The results show an ablation behaviour comparable with the reference material copper. With an applied fluence of 13 J/cm² all metals show an increasing ablation rate for small scan velocities caused by an enhanced pulse to pulse interaction as shown in fig 11. Despite its high reflectivity in the near-infrared and its high boiling point copper has the highest ablation rate of all tested metals. A main difference was observed in the bottom of the ablated cell or area. The material copper and Nickel did not show any artefacts at the cell bottom (Fig. 7c).

In the case of stainless steel X 1.4310 and steel St-52 surface defects, so called cone like protrusions CLPs [3] are emerging on the ablated area like clusters. The formation of the CLP starts at some nucleation of the surface (Fig. 12a). During further laser ablation the clusters of CLP are formed and grow until the complete area of the ablation

zone is covered. The pulse to pulse overlap, adjusted with the surface speed at constant pulse repetition rate of 2 MHz has an influence on the growth of the CLP clusters as demonstrated in Fig. 12 a) 12 b) and 12 c). The CLP area in the ablation zone expands, with decreasing pulse to pulse distance.

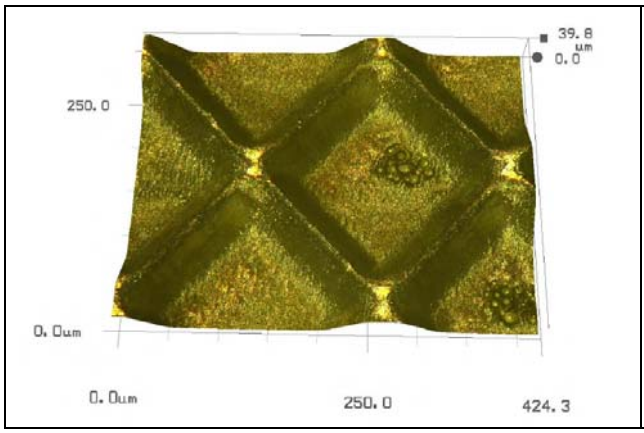

Fig. 12 a) stainless steel, 18m/s

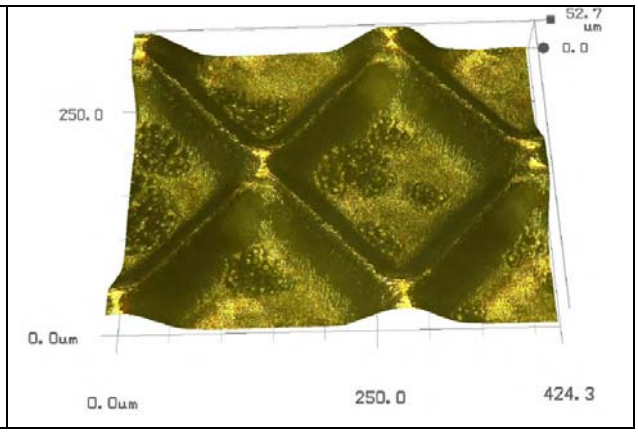

Fig. 12 b) 15m/s

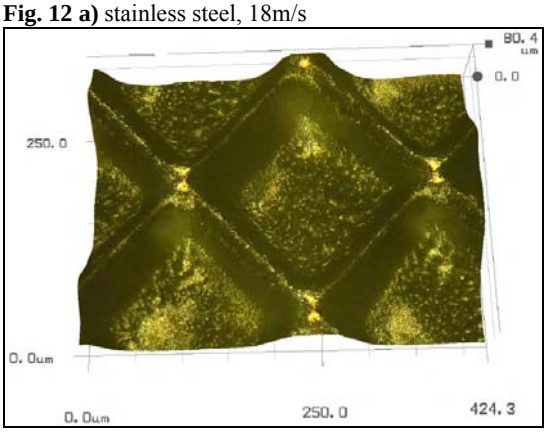

Fig. 12 c) 12m/s

The phenomenon was as well observed at some Aluminium alloys e.g. AlMg3. The CLP phenomenon causes a reduced resolution, a higher surface roughness and disturbs the layer based 3D ablation. If this process has been started once, it could not be stopped by a parameter change of the ultrashort pulse laser. Two different nucleation factors can be stated, an amorphous structure of the material or a locally higher surface roughness.

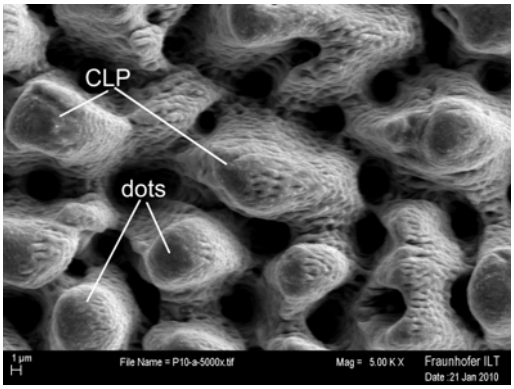

Fig. 13 Dots and CLP (SEM picture), [4]

3.2 Pulse separation by a "Cross-Scan" technique

As a second method of fast pulse separation the cross scan technique was investigated as described in Chapter 2.2 and Fig 5. The synchronisation of the pulses (pixels) in a cross scan line according to the circumferential position of the cylinder is controlled by an electronic board in combination with a control software. The cross scan time t and the cross scan length l define the scan velocity. In a cross scan cycle the pulses of the ps laser source are selected by the pulse picker in correlation to the deflection angle Θ and controlled by the digital data set.

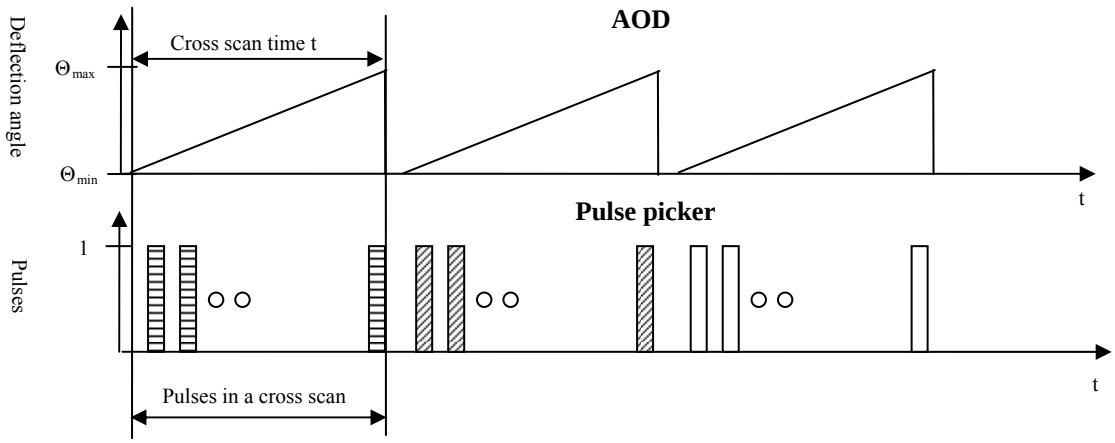

Fig. 14 time – angle/pulse diagram for a pulse picker – deflector arrangement

The time schedule given in the diagram Fig. 14, is space resolved shown in Fig. 15. The pulse picker is synchronised with the two axis of the AOD deflection angle and the circumference movement of the cylinder. The first cross scan cycle is symbolised by 3 consecutive dots. The second cross scan cycle is symbolised by the next 3 dots. The feed between the cross scan lines is defined by the circumferential surface speed. The feed between the cross scan multiplets is defined by the slow axial movement of the laser beam.

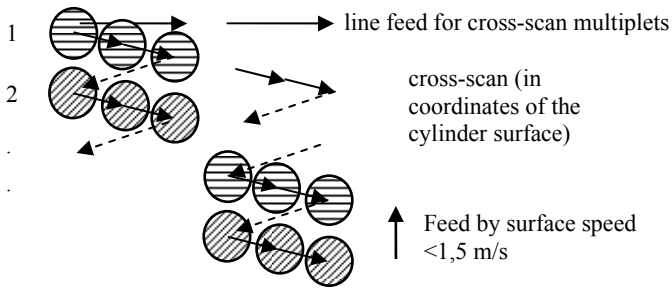

Fig. 15 cross-scan algorithm resolved on the work piece

The cross-scan line approach leads to patterning with separated laser spots, where each laser spot is positioned adjacent to the former one.

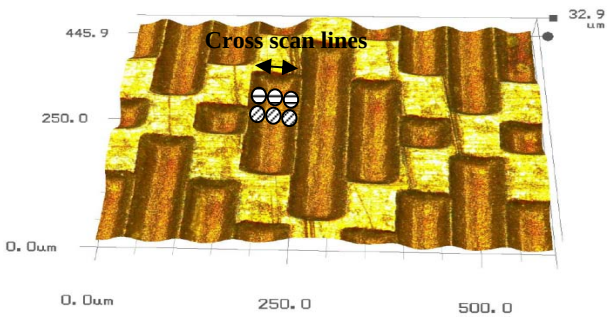

Fig. 16 Ablated cell with cross-scan, Cu, depth 25µm

In Fig. 16 the line feed in axial direction of 90µm is combined with an effective cross scan length of 80µm. As result a wall between the cross scan lines is visible. The cross scan algorithm demonstrated in Fig. 15 is applied.

At a constant cylinder surface speed of 1.3m/s, a pulse repetition rate of 2 MHz, and a fluence of 22 J/cm² Fig. 17 shows the ablation rates for different cross scan frequencies. As the ablation rate and the ablation quality is impacted by the pulse to pulse overlap the cross scan frequency has to be optimised with respect to the pulse to pulse distance along the cross scan line and with respect to the cross scan to cross scan distance. At lower scan frequencies the scan velocity is slow, meaning the pulse to pulse overlap is large resulting in enhanced ablation rate. At a pulse repetition rate of 2 MHz the optimum working condition is in a frequency range from 170KHz to 290KHz. In this range the pulse to pulse and the cross scan line to line distance shows an optimal distribution (Fig. 18). Increasing of the cross scan frequency provides a faster scan with reduced pulse to pulse overlap. With this enlarged pulse to pulse distance the pre-heating effect is decreased and the ablation rate is reduced.

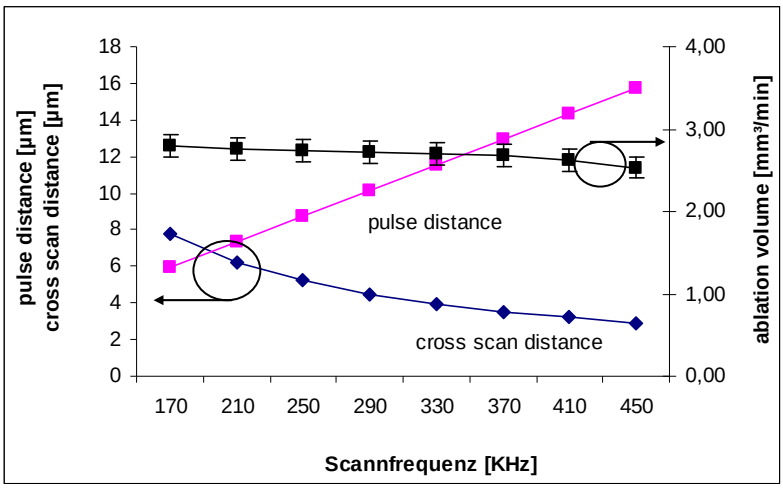

Fig. 17 scan frequency / pulse and cross scan distance / ablation rate, Cu

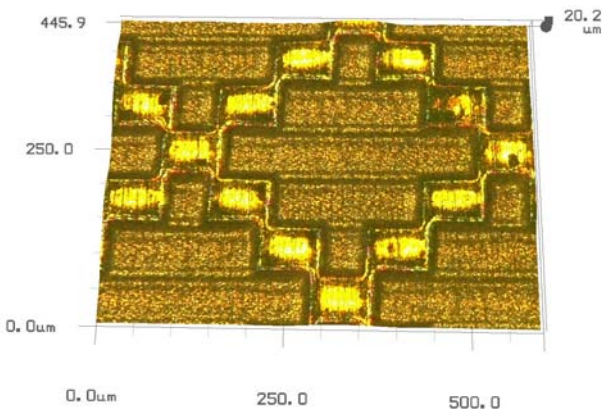

Fig. 18
Cu
pulse repetition rate: 2MHz
Surface speed: 1,3m/s
Cross-Scan frequency: 210KHz
Distance cross scan line to cross scan line: 6µm
Pulse overlap: 20%
Fluence: 22 J/cm²
Magnification: x500

4. Conclusions

Using two different scanning techniques, laser ablation of different metal surfaces has been investigated with a high repetitive ps-laser for ablation quality and efficiency. The pulse to pulse overlap has a significant impact on both, quality and productivity. Two regimes can be identified: a thermal and a minor thermal regime. A higher pulse overlap results in an increase of thermal effects (debris, molten parts, oxide layers). The optimum pulse overlap with highest minor-thermal efficiency is defined by the border line between these two regimes (Fig. 8). The comparison of the ablation characteristics of different metals shows material dependent precision and ablation rates. Material dependent artefacts (cone-like-protrusions and holes) could be identified which have an impact on the ablation quality [3].

The experience gained with this study has finally been transferred to an ablation algorithm of 3D freeform engraving in metal surfaces (Fig. 19).

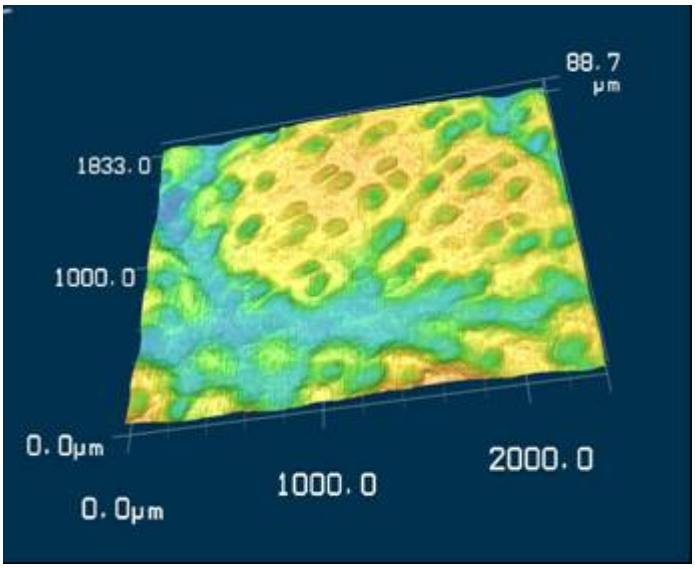

Fig. 19 3D Digital free form "leather" ablated in 255 2D-layers, Cu, depth 120µm

Acknowledgements

This work was partly funded by the BMBF within the frame program MABRILAS / PIKOFLAT.

References

1. B. Neuenschwander, G. Bucher, G. Hennig, Ch. Nussbaum, B. Joss, M. Muralt, S. Zehnder, U. Hunziker, P. Schuetz: „*Processing of dielectric materials and Metals with ps-laserpulses*" 2010 ICALEO Conf. Proc. M101
2. J. Koenig, S. Nolte, A. Tuennermann*: "Plasma evolution during metal ablation with ultra short laser pulses"*, Optics Express 13, p. 10597 – 10607, 2005
3. M Tsukamoto et al.:*"Microstructures formation on titanium plate by femtosecond laser ablation"*, 2007 J. Phys.: Conf. Ser. 59 666, doi: 10.1088/1742-6596/59/1/140
4. S. Eifel, A. Dohrn, A. Gillner: „Quality Aspects in High Power Ultra Short Pulse Laser Ablation", Proceedings of LPM2010, Stuttgart 2010
5. P. Manion, J. Magee, E. Coyne, G. M. Oconnor: "Ablation threshold in ultrafast laser micro-machining of common metals in air", SPIE Vol. 2873, 2003
6. C.A Hartmann, T. Fehr, M. Brajdic, A. Gillner: „Investigation on Laser Micro Ablation of Steel Using Short and Ultrashort IR Multipulses", JLMN-Journal of Lasre Micro/Nanoengineering Vol. 2, No. 1, 2007